RSC Advances

RSC Advances

www.rsc.org/advances

ROYAL SOCIETY
OF CHEMISTRY

www.rsc.org/advances

Journal Name

RSC Advances

Dynamic Article Links ▶

ARTICLE TYPE

Degradation performance of Keggin Type Zn-Mo-Zr catalyst for acidic green B with ultrasonic waves

Zhihong Zhang*[a], Zhipeng Liao[b],Gehong Zhang[b]

A new heteropolyacid salt, $Na_6[Zn(Mo_{11}ZrO_{39})]•20H_2O$ with Keggin structure of 1:1:11 series, was synthesized via classic acidification method, and characterized by inductive coupled plasma atomic emission spectroscopy (ICP-AES), fourier transform infrared spectroscopy (FT-IR), ultraviolet spectra (UV), X-ray diffraction (XRD), thermogravimetric analysis/ differential scanning calorimetry (TGA/DSC)
10 and A KY-AMRAY 1000B scanning electron microscope (SEM). Acidic green B (AGB) was applied to exam the degradation performance of the catalyst which affect with ultrasonic waves. The effects of operating parameters, such as catalyst dosage, ultrasonic power, media ultrasonic frequency, dye initial concentration and pH value on degradation were discussed. In the experiment, the degradation rate ran up to 95.72% under the optimum conditions i.e. a dosage of the catalyst of 0.8 $g•L^{-1}$, a concentration of the
15 AGB of 10 $mg•L^{-1}$, a ultrasonic frequency of 45 kHz and a ultrasonic power of 100 W in just 60 minutes.

1. Introduction

With the deterioration of the environment, increasing serious pollution problem has greatly attracted the attention of human beings. Water resources, especially available water resources are
20 fewer day by day because of the pollution, so it is essential to find some effective ways for the wastewater treatment. Textile effluents contain a large quantity of organic dye compounds, which can bring serious environmental problems owing to their poor biodegradability, toxicity and carcinogenicity [1-5]. Physical
25 adsorption and microbiological discoloration are two master traditional methods to reduce synthetic dye molecules [5-9], but both of them have certain limitations [5, 6, 10-13].

Heteropolyacid (salts) belongs to a prodigious class of chemical substances which behave preeminent in some areas.
30 Excellent transmission and reserve capacity of electrons and protons, high activity of "lattice oxygen" and great proton acid, all these bring up versatile properties of heteropolyacid (salts), such as acidic and redox properties. Due to these splendid properties, heteropoly compounds have received much attention
35 for many years [14]. Many works have been done to correlate these properties with catalytic actions. Recently, significant efforts have been addressed to apply such compounds to organic synthesis [15], pharmaceutical chemistry, electrolyte and surface promoters for low temperature fuel cells [16-18], wastewater
40 treatment and other fields. In the experiment, the anion of catalyst, $[Zn(Mo_{11}ZrO_{39})]^{6-}$, is made from the replacement of molybdenum

----

[a] School of Materials and Chemical Engineering, Xi'an Technological University, Xi'an 710021, China.
45 [b] School of Civil Engineering, Xi'an Technological University, Xi'an 710021, China.

by zinc in the peripheral metal atom positions of the 1:12 series
$[ZrMo_{12}O_{40}]^{4-}$, the structure is consistent after the replacement of
50 molybdenum, Fig. 1 shows the structure of $[Zn(Mo_{11}ZrO_{39})]^{6-}$, the purple atom at the center of the anion is zirconium, the center of the octahedral atoms are molybdenum.

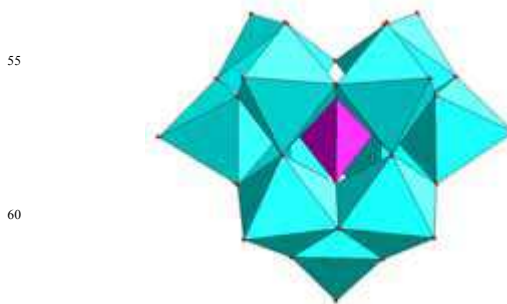**Fig.1** Structure of $[Zn(Mo_{11}ZrO_{39})]^{6-}$

65 Better operating conditions, stronger oxidation ability, the capability of completely degrading pollutants without secondary pollution, all these advantages belong to heteropolyacid (salts) photocatalytic oxidation method. In view of the advantages mentioned above, heteropolyacid (salts) has been considered as a
70 kind of favourable catalysts to catalytic the degradation of organic wastewater [19, 20]. Nevertheless, for the deep chromaticity and high turbidity of dye wastewater, the effect of light transmission should be considered, which may lead to the drop of degradation rate. Many researchers have concentrated on
75 the actual application of ultrasonic waves in degradation of organic pollutants [21-26], however, currently, fewer have concerned on the combination of heteropolyacid (salts) and ultrasonic waves to degrade the organic wastewater, this research is still in the initial stage. The weakness of transmission about

Tab. 1 Chemical analysis of the catalyst

HPS	Zr	Mo	Zn	Zn: Zr: Mo
ZnZrMo	3.82 (3.90)	44.75 (45.24)	2.73 (2.78)	1.00: 1.00: 11.10

photocatalytic method mentioned above does not exist for ultrasonication, even in water medium, penetration of ultrasonic waves is generally up to 15-20 cm. In the general case, those chemical reactions catalyzed by light can also be managed by ultrasonic waves. Through access to large amounts of literatures, the degradation principle of ultrasonic waves can be classified into the following two mechanisms: One is the sonoluminescene mechanism, sonoluminescence is a phenomenon that occurs when a small gas bubble is acoustically suspended and periodically driven in a liquid solution at ultrasonic frequencies, resulting in bubble collapse, cavitation, and light emission. The thermal energy released from the bubble collapse is so great that it can cause weak light emission [27], so the light generated may employ the heteropolyacid (salts) serve as photocatalysts; another is high excitation mechanism, acoustic cavitation can cause the formation, growth and implosive collapse of bubbles in the liquid, the collapse of bubbles generates localized "hot spot" with transient temperatures of about 5000 K and pressure levels of about 1000 atm [24], under such extreme conditions, water molecules inside bubbles dissociate into •OH, yet the efficiency is very low. If heteropolyacid (salts) gets the energy from ultrasonic waves, it will lead to the escape of oxygen atom from lattice and the appearance of "holes", the presence of the "holes" can result in the generation of more • OH. The degradation mechanism of the catalyst is described in Fig. 2, it is easy to find that this degradation mechanism is similar to the mechanism of TiO_2 photocatalyst.
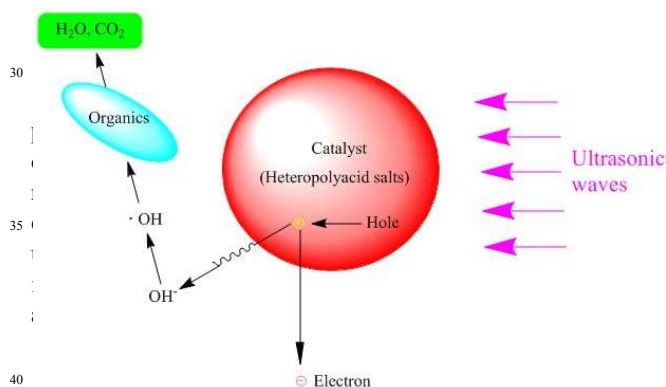

Fig. 2 Mechanism of the catalyst

In this paper, a novel heteropolyacid salt, ZnMoZr, has been synthesized, the structure and ultrasonic catalytic degradation performance under different conditions were cognized, the degradation kinetics of AGB were also studied in this work.
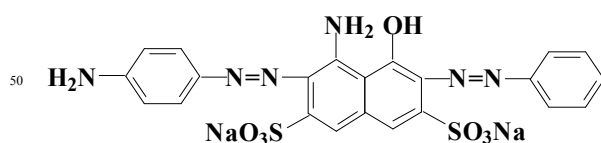

Fig. 3 Structural fomula of AGB

2. Experimental

All the chemicals were purchased from Keluo (China) of analytical grade and used as received without further purification. Deionized (DI) water was used throughout the whole experiment.

Synthesis of ZnZrMo

$Na_2MoO_4•2H_2O$ (0.044 mol) was dissolved in H_2O (200 ml) and the pH value of solution was adjusted to 6.5 with acetic acid. Then a solution of $ZnCl_2•8H_2O$ (0.004 mol) in H_2O (20 ml) was added drop wise under magnetic stirring. When the white precipitation was appeared, readjusted the pH of solution to 5.5 and continued stirring until the solution became clarification at the temperature of 70°C. And a solution of $ZnCl_2$ (0.004 mol) in H_2O (20 ml) was added drop wise with boiling-reflux for 1-2 h. The product was purified by the recrystallization method and dried at the room temperature. The ZnZrMo heteropolyacid salt was the colorless powder.

3. Results and discussion

3.1. Elemental analysis

The molar ratio of elements was examined by HK-2000 inductive coupled plasma atomic emission spectroscopy (ICP-AES). As shown in Table. 1, the ICP-AES analysis shows that the mole ratio of Zn: Zr: Mo is close to 1:1:11 (Data in the bracket is theoretical), which indicates the catalyst belongs to 1:1:11 series of heteropolyacid salt.

3.2. TGA/DSC analysis

The thermogravimetric analysis/ differential scanning calorimetry (TGA/DSC) study was carried out using Mettler Toledo TGA/DSC 1 equipment in a dynamic argon atmosphere at the range of 25-600°C, and the heating rate was 15°C per minute. As shown in Fig. 4, the weight of catalyst decreases from 74°C to 400°C, but after 400°C, the weight of catalyst remains constant. There are four endothermic peaks (74, 105, 325 and 400°C)
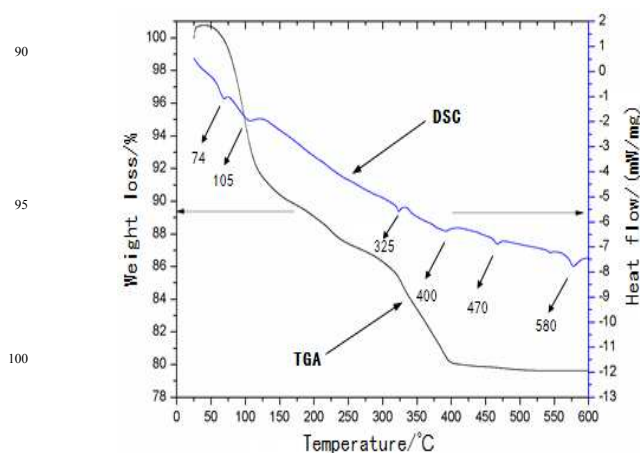

Fig. 4 TGA/DSC curves of catalyst

in the DSC curve, three major weight loss stages are divided by these four peaks. In the first stage, the weight loss is 5.4%, the lost components are mainly small molecules such as physically absorbed water and acetic acid. In the second stage, the weight loss is 9.4%, equivalent to lose thirteen crystallization water. In the third stage, the weight loss is 4.8%, corresponding to lose seven crystallization water. The endothermic peaks at 470°C and 580°C are assigned to the structure collapse of catalyst. It can be concluded from Fig. 4 that the sample is examined as an outstanding catalyst which possesses favorable thermal stability. Besides, the molecule formula of the catalyst can be summarized as $Na_6[Zn(Mo_{11}ZrO_{39})]\cdot20H_2O$.

3.3. FT-IR and UV analysis

The fourier transform infrared spectroscopy (FT-IR) was recorded on a Nicolet Nexus spectrometer in the region 700-4000 cm^{-1} using KBr pellets. The characteristic vibration bands of the heteropolyacid salts with Keggin structure appear in the range of 700-1100 cm^{-1}. As shown in Fig. 5, four characteristic bands can be observed: 1020 cm^{-1} (Zr-Oa), 943 cm^{-1} (Mo=Od), 877 cm^{-1} (Mo-Ob-Mo) and 771 cm^{-1} (Mo-Oc-Mo)(Oa-oxygen in the central ZrO_4 tetrahedron, Od-terminal oxygen bonding to Mo atom, Ob-edge-sharing oxygen connecting Mo and Oc-corner-sharing oxygen connecting Mo_3O_{13} units), all of which can be detected for the Keggin anion. Besides, the band at 910 cm^{-1} is attributed to the symmetric stretching of Mo=O bonds, the band at 1410 cm^{-1} could be attributed to the stretching vibration of C-O bonds or In-plane bending vibration of O-H bonds. In high frequency region, the band at 1340 cm^{-1} might be assigned to the bending vibration of C-H bonds. In addition, the band at 1560 cm^{-1} could be caused by carbonyl group. Meanwhile, there are other bands at 1640 cm^{-1} and 3430 cm^{-1}, which orderly assigned to the bending vibration of O-H bonds and the stretching vibration of H-O-H bonds of absorbed water. The appearance of carboxyl group and C-H bonds is owing to the residue of glacial acetic acid or its salts. The flerry of the stretching vibration band is mainly owing to the large size of zirconium ions, which may cause the relaxation and small cohesion of the molecular, so that the change of relative chemical bond vibration is obviously.
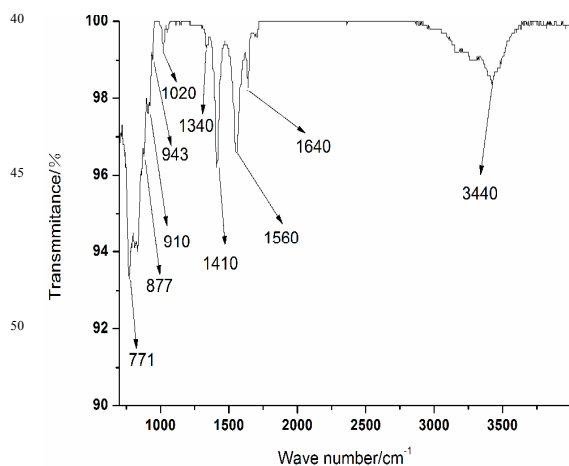

Fig. 5 FT-IR spectra of catalyst

The ultraviolet spectrum (UV) was measured on a Shimadzu

UV-2500 spectrophotometer from 200 to 400 nm. The UV spectra of 1:1:11 series of Keggin type heteropolyacid (salts) generally possesses two strong characteristic absorption peaks, the absorption peak with higher energy belongs to double bond character, which is in the vicinity of 200 nm, and the absorption peak with lower energy attributes to bond property, which is at about 260 nm. As in Fig. 6, the peaks at 208 nm and 253 nm are orderly assigned to Od→Mo and Ob/ Oc→Mo charge transfer, both of them are in accordance with the UV spectra of 1:1:11 series of Keggin type heteropoly compounds.
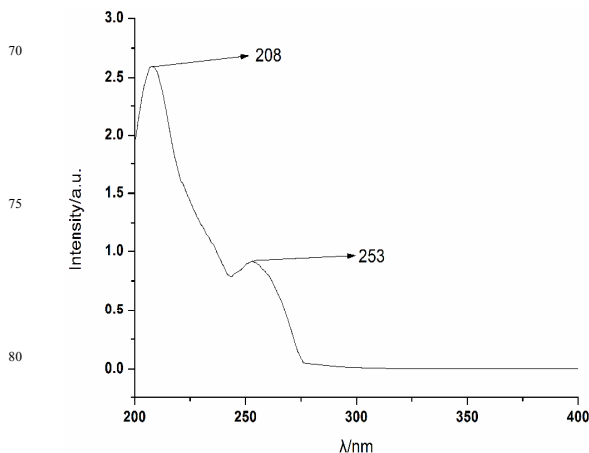

Fig. 6 UV absorption spectrum of catalyst

3.4. XRD and SEM analysis

X-ray powder diffraction analysis (XRD) was obtained on a Shimadzu XRD-6000 X-ray diffractometer. The instrument was equipped with a Cu tube operated at 40 kV and 30 mA, diffraction data were collected in the 5-40° 2θ range with a step size of 0.02 at a rate of 4° per minute. There are four characteristic peaks (2θ is in 7~13°, 16~23°, 25~30° and 31~38°) in the XRD pattern of 1:1:11 series of Keggin type heteropolyacid (salts). Fig. 7 depicts the XRD pattern of the catalyst, the unfolded peaks (2θ = 10.18°, 18.86°, 29.2° and 34°) are consistent with characteristic peaks of 1:1:11 series of Keggin type heteropoly compounds. Integrate the patterns of TGA/DSC, FT-IR, UV and XRD, the catalyst is demonstrated to be a kind of Keggin type heteropoly compounds.
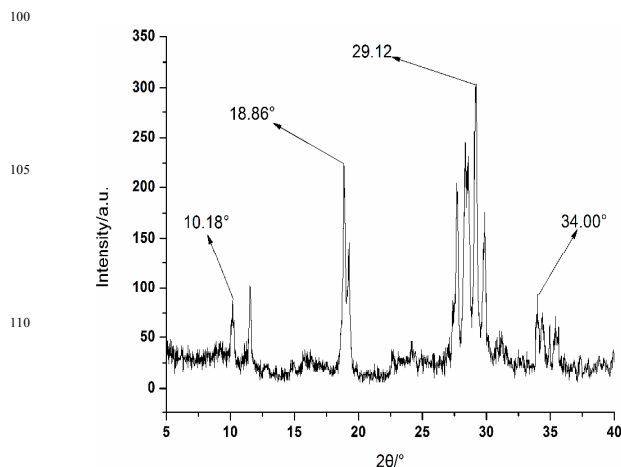

Fig. 7 XRD pattern of catalyst

The surface morphologies of catalyst were obtained by a KY-AMRAY 1000B Scanning electron microscope (SEM) (Fig. 8 a and b). Fig. 8 shows that the sample particles are honeycomb in low magnification, and appear regular hexahedron shape in high magnification. Although the size of the sample particles is not consistent, the shape of the sample particles is almost the same. In addition, it can be clearly seen that the particle size is basically less than 3 μm as presented.
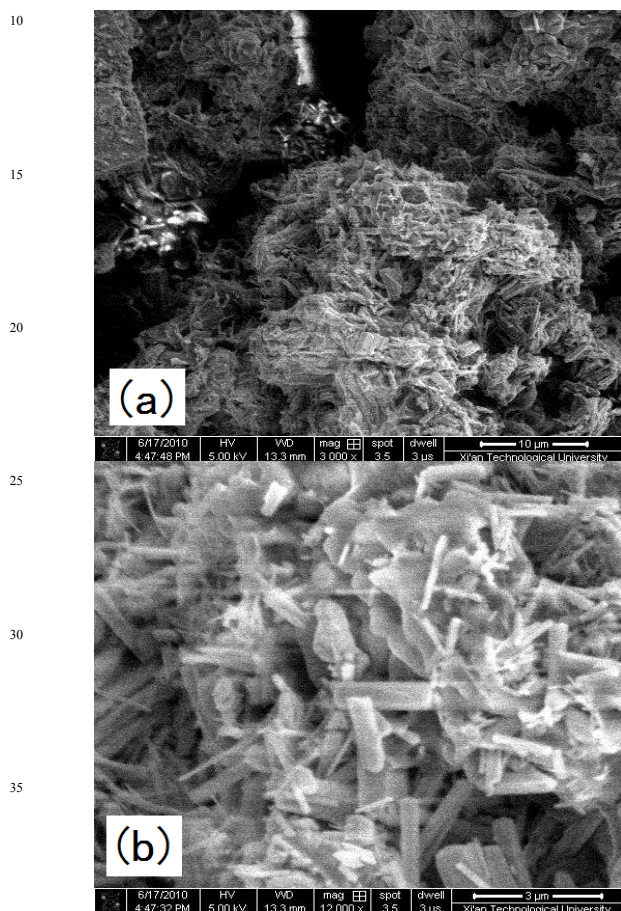

Fig. 8 SEM images of catalyst: (a) Low magnification, (b) High magnification

3.5. Ultrasonic degradation property analysis

Analysis method: The maximum absorbance of AGB is at 605 nm, the absorbance of the following experiment is measured at this wave number. The degradation rate could be described as the following equation according to the Lambert-Beer law:

$$\text{Degradation rate (\%)} = [(A_0 - A)/A_0] \times 100\% \qquad (1)$$

Where A_0 is the absorbance of initial AGB dye wastewater before ultrasonic catalytic treatment, A is the absorbance of AGB dye wastewater irradiated by ultrasonic waves after t minutes.

3.5.1. Effect of different dosage of catalyst on the catalytic activity

The dosage of catalyst was chosen from 0.0 g•L^{-1} to 1.0 g•L^{-1}, and kept the AGB dye wastewater (100 ml, 10 mg•L^{-1}) irradiated by a 45 kHz and 80 W ultrasonic waves. As in Fig. 9, in the first 20 minutes, the highest degradation rate achieved when the dosage was 0.6 g•L^{-1}, but after 20 minutes, the degradation rate of 0.8 g•L^{-1} was the highest. As a result, if the reaction time is less than 20 minutes, the dosage of 0.6 g•L^{-1} should be taken into the consideration, while the reaction time is more than 20 minutes, the dosage of 0.8 g•L^{-1} would be the best choice. The following experiments were conducted more than 20 minutes, therefore, 0.8 g•L^{-1} was selected. Fig. 9 shows that the degradation rate increased up to tiptop 95.72% after 60 minutes when the dosage was 0.8 g•L^{-1}. Through the experiment can also find that when the dosage of catalyst is controlled in a certain range, degradation rate is increased with the increasing dosage, but more than a certain value, the increase of degradation rate is not obvious, which is mainly because as more catalysts added into the solution, side reaction might be easily access to take on. At the same time, superfluous catalysts might shield each other, and this would minish the acoustic effect of ultrasonic waves, finally, the degradation rate might be affected.
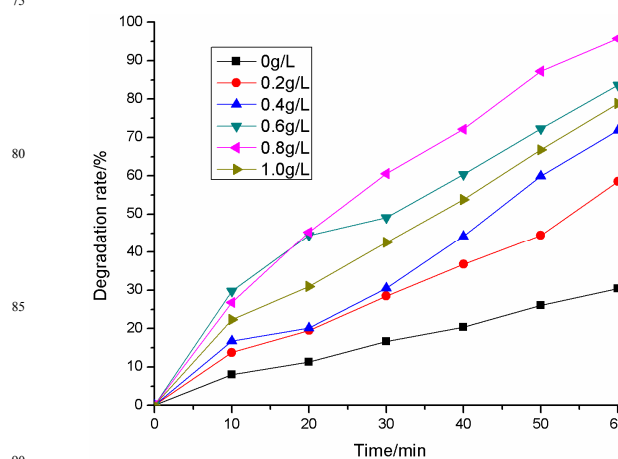

Fig .9 Effect of catalyst dosage

3.5.2. Effect of different initial concentration of dye wastewater on the catalytic activity

The initial concentration of the wastewater was chosen from 10 mg•L^{-1} to 50 mg•L^{-1}, and kept the solution irradiated by a 45 kHz and 80 W ultrasonic waves 60 minutes, the corresponding final degradation rates were 95.72%, 88.60%, 75.07%, 60.65% and 57.24%, the catalyst shows the highest catalytic activity when the initial concentration was 10 mg•L^{-1}, therefore all the following experiments were conducted at this concentration. Fig. 10 states that with the increasing of initial concentration, the degradation rate decreased, but the degradation quantity increased relatively. This is mainly because when the dosage, ultrasonic frequency and power remain the same, and keep the system at low concentrations, the number of cavitation bubbles, •OH and other free radicals will remain relatively stable, the possibility of degradation reaction and the concentration of reactant is proportional, therefore, total removal of AGB dye molecules increases with the rising initial concentration in per unit volume and per unit time. However, with the increase of initial concentration, dye molecules and transient products on cavitation bubble surface tend to be saturated, which may hinder the spread of free radicals outside the bubbles and reduce the reaction region. In the meantime, the reaction region may be occupied by

the transient products, and the reverse reaction of degradation is probably to be expedited owing to the excessive transient products [28].
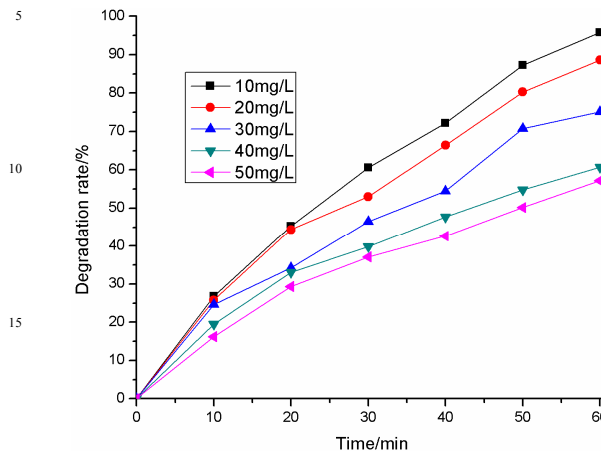

Fig. 10 Effect of AGB initial concentration

3.5.3. Effect of different pH of dye wastewater on the catalytic activity

Due to the fact that pH value has a very important effect on catalytic activity [29], influence of different pH value on ultrasonic catalytic activity was investigated. The pH value of solutions (1, 3, 5, 7 and 9) was adjusted by sodium hydroxide and hydrochloric acid solution, and kept the solutions irradiated by a 45 kHz and 80 W ultrasonic waves 60 minutes, the final corresponding degradation rates (52.63%, 73.81%, 92.17%, 91.86% and 76.87%) appears in Fig. 11. Obviously, the degradation rate was the highest when the initial pH value of dye wastewater was 5.0, thus the pH values of the following experiments were controlled at 5.0. It can be clearly seen that when the pH value of the solution was controlled in neutral or weak acid, the degradation rate was relatively higher. This is mainly because pH value can effect the form of heteropolyacid salts and dissociation of dye molecules. Dye molecules exist in molecular form in acid solution, they can accumulate on the
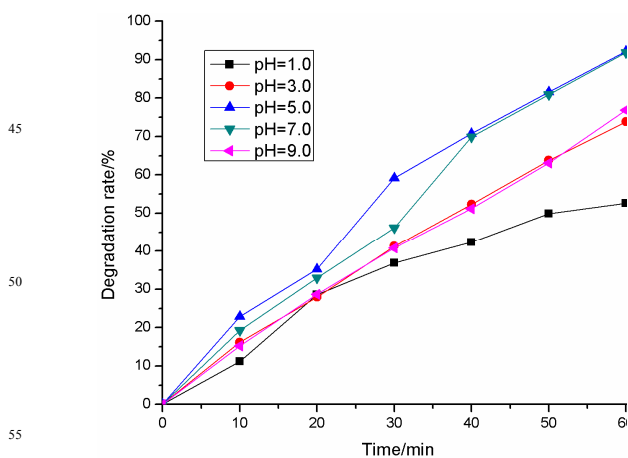
cavitation bubble surface or volatilize into the cavitation bubbles, however, a strong acid environment may lead the H^+ in solution to expend part of •OH, the degradation reaction would be affected; dye molecules only exist in the form of ion in alkaline solution, it is difficult for ions accumulating on the cavitation bubble surface or volatilizing into the cavitation bubbles, reactions only take place in the gas-liquid interface, which is unbeneficial to the degradation reaction. On the other hand, heteropolyacid salts only exist in neutral or weak acid, they will decompose in other conditions and lose the catalytic activity. Under the experimental condition, when the added amount of the catalyst was 0.8 g•L^{-1}, the acidity of the solution was just within the best range, therefore, there was unnecessary to adjust the acidity of the solution.

3.5.4. Effect of different ultrasonic frequency on the catalytic activity

The ultrasonic power was controlled at 80 W and the ultrasonic frequency was adjusted to 28 kHz, 45 kHz, 80 kHz and 100 kHz respectively. As in Fig. 12, the highest degradation rate attained 95.72% when the ultrasonic frequency was 45 kHz, thus the ultrasonic frequency of the following experiment was fixed at 45 kHz. It can be concluded from Fig. 12 that, as other conditions remain unchanged, there is an optimum frequency, but this frequency is not the highest or the lowest. This is mainly because the radius of cavitation bubbles at low frequency is larger than that at high frequency, as a result, the collapse time at low frequency is longer than that at high frequency. However, high frequency leads to the shorter time of collapse, and there will be more chances for •OH to escape from the cavitation bubbles, which may avoid the free radicals recombining with each other in the bubbles, thus high frequency can promote the degradation. While high frequency can also lead to the drop of cavitation intensity and accelerate the decay of liquid energy, which may cause the cavitation process difficult to occur and decrease the amount of •OH, thereby the degradation rate may be affected. The best frequency of degradation activity emerges with both actions mentioned above.
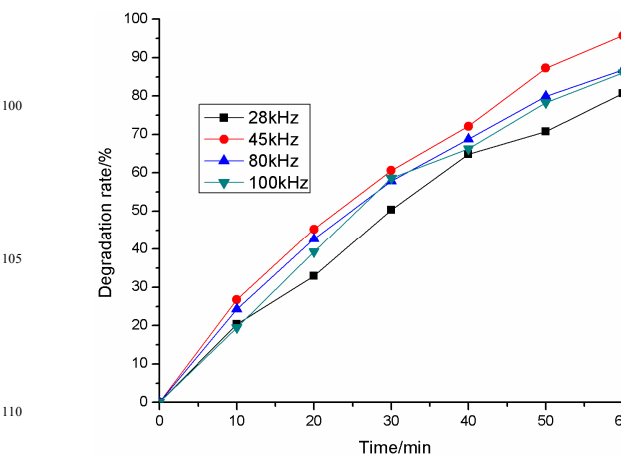

Fig. 12 Effect of ultrasonic frequency

3.5.5. Effect of different ultrasonic power on the catalytic activity

Fig. 11 Effect of initial pH

Tab. 2 Kinetic parameters of pseudo-first order equation

Initial concentration (mg·L^{-1})	Rate constant (min^{-1})	Half-life period (min)	linear coefficients R^2
10	0.02374	29.20	0.98179
20	0.01822	30.05	0.99558
30	0.01850	37.47	0.99011
40	0.01615	42.92	0.99450
50	0.01436	48.27	0.99580

The power of ultrasonic waves was dominated as 40 W, 60 W, 80 W and 100 W respectively. Fig. 13 shows that when the power of ultrasonic waves was 100 W, the greatest effect appeared, the degradation rate rose up to 95.72%. Apparently, it also can be seen that the degradation rate increases with the increasing power. This is mainly because the reinforce of ultrasonic power adds to the number of "cavitation nucleus" and strengthens the effect of cavitation pyrolysis on the pollutants [30, 31]. At the same time, the oxidation of •OH and other free radicals is also enhanced, therefore, ultrasonic degradation was promoted. Nevertheless, excessively strong power intensity may be counterproductive. When the system accepts excessively high acoustic energy, the cavitation bubbles will get very big in sonic negative phase and form acoustic shielding, which may decrease the available acoustic energy in the reaction.
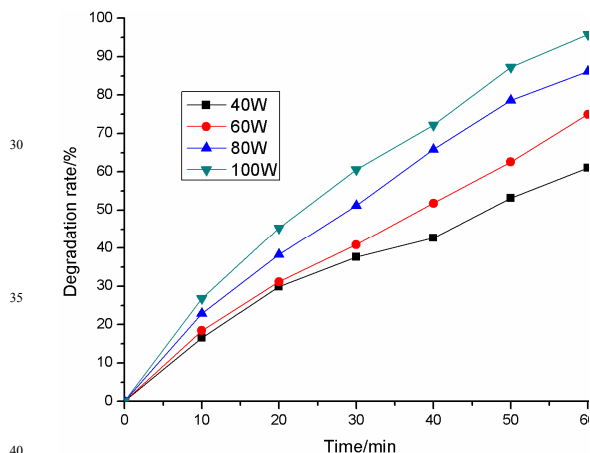
**Fig. 13** Effect of ultrasonic power

3.5.6. Degradation kinetics

Ultrasonic catalytic oxidation tests were carried out with different concentrations of AGB dye wastewater to investigate the kinetics of ultrasonic catalytic degradation of AGB with catalyst. The experiment data can be described by the pseudo-first order equation:

$$\ln \frac{C_0}{C_t} = kt \qquad (2)$$

Where C_0 is the initial concentration of AGB (mg·L^{-1}), Ct is the concentration of AGB at t minutes (mg·L^{-1}) and k (min^{-1}) is the pseudo-first order rate constant. 0.8 g·L^{-1} catalyst was put into AGB dye wastewater, the ultrasonic frequency was 45 kHz and the power of ultrasonic waves was 100 W.

Fig. 14 shows the degradation kinetics curves of AGB over the catalyst during irradiation time. Obviously, the degradation
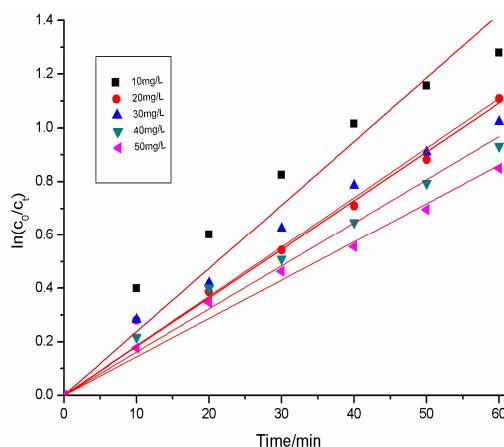
Fig. 14 Kinetic characters of ultrasonic degradation of AGB at different initial concentrations, pseudo-first order model fit

rate of AGB dye wastewater decreases with the increase of initial concentration. It can be concluded from Table. 2 that, the linear coefficients (R^2) of curves draw by ln (C_0/C_t) plotted against time are almost more than 0.99, which indicates that the degradation process is basically in accord with the pseudo-first order kinetic model.

Conclusions

We have successfully synthesized a novel heteropolyacid salt Na$_6$[Zn(Mo$_{11}$ZrO$_{39}$)]·20H$_2$O. The catalyst possesses complete Keggin structure and has a good thermal stability. The molar ratio of elements of the catalyst is 1:1:11. In the experiment, the degradation performance of catalyst with ultrasonic waves is excellent, the degradation rate reached 95.72% under the optimum conditions. Besides, the degradation of AGB dye wastewater by the catalyst with ultrasonic waves is well adhered to the pseudo-first order kinetic model.

Acknowledgements

References

1 S. Sathian, M. Rajasimman, G. Radha, V. Shanmugapriya, V. Shanmugapriya and C. Karthikeyan, *Alex. Eng. J.,* 2014, **53**, 417

2 K. Zhao, G. Zhao, P. Li, J. Gao, B. Lv and D. Li, *Chemosphere.,* 2010, **80**, 410

3 R. G. Saratale, G. D. Saratale, J. S. Chang and S. P. Govindwar, *Biodegradation.,* 2010, **21**, 999

4 E. E. Baldez, N. F. Robaina and R. J. Cassella, *J. Hazard. Mater.,* 2008, **159**, 580

5   E. Forgacs, T. Cserhátia and G. Orosb, *Environ Int.,* 2004, **30**, 953

6   L. Lucarelli, V. Nadtochenko, and J. Kiwi, *langmuir.,* 2000, **16**, 1102

7   M. T. Yagub, T. K. Sen, S. Afroze and H. M. Ang, *Adv. Colloid Interface Sci.,* 2014, **209**, 172

8   V. K. Guptaa and Suhasb, *J. Environ. Manage.,* 2009, **90**, 2313

9   E. J. Almeida and C. R. Corso, *Chemosphere.,* 2014, **112**, 317

10   M. Tichonovas, E. Krugly, V. Racys, R. Hippler, V. Kauneliene, I Stasiulaitiene and D Martuzevicius, *Chem. Eng. J.,* 2013, **229**, 9

11   S. U. M. Khan, M. Al-Shahry and W. B. Ingler Jr, *Sci.,* 2002, **297**, 2243

12   C. Bauer, P. Jacques and A. Kalt, *J. Photochem. Photobiol., A.,* 2001, **140**, 87

13   I. Justicia, P. Ordejón, G. Canto, J. L. Mozos, J. Fraxedas, G. A. Battiston, R. Gerbasi and A. Figueras, *Adv. Mater.,* 2002, **14**, 1399

14   P. Souchay, *Ions minéraux condensés. Masson, Paris.*, 1969.

15   K. Nowińska, A. Wącław, M. Sopa and M. Klak, *Catal. Lett.,* 2002, **78**, 347

16   N. Giordano, P. Staiti, S. Hocevar and A. S. Arico, *Electrochim. Acta.,* 1996, **41**, 397

17   A. S. Aricò, E. Modica, I. Ferrara and V. Antonucci, *J. Appl. Chem.,* 1998, **28**, 881

18   A. S. Aricòa, H. Kim, A. K. Shuklab, M. K. Ravikumarc, V. Antonuccia and N. Giordanoa, *Electrochim. Acta.,* 1994, **39**, 691

19   I. V. Kozhevnikov, *Chem. Rev.,* 1998, **98**, 171

20   S. Antonaraki, E. Androulaki, D. Dimotikali, A. Hiskia and E. Papaconstantinou, *J. Photochem. Photobiol., A.,*2002, **148**, 191

21   P. Ning, H. J. Bart, Y. J. Jiang, A. D. Haan and C. Tien, *Sep. Purif. Technol.,* 2005, **41**, 133

22   L. Jiang, S. Y. Guo and X. N. Li, *Polym. Degrad. Stab.,* 2005, **89**, 6

23   S. G. Ostlund and A. M. Striegel, *Polym. Degrad. Stab.,* 2008, **93**, 1510

24   X. K. Wang, Y. C. Wei, C. Wang, W. L. Guo, J. G. Wang and J. X. Jiang, *Sep. Purif. Technol.,* 2011, **81**, 69

25   X Wang, L. G. Wang, J. B. Li, J. J. Qiu, C. Cai and H. Zhang, *Sep. Purif. Technol.,* 2014, **122**, 41

26   A. Ghauch, H. Baydoun and P. Dermesropian, *Chem. Eng. J.,* 2011, **172**, 18

27   M. P. Brenner, S. Hilgenfeldt and D. Lohse, *Rev. Mod. Phys.,* 2002, **74**, 425

28   I. Hua and M. R. Hoffmann, *Environ. Sci. Technol.,* 1997, **31**, 2237

29   T. E. Agustina, H. M. Ang and V. K. Vareek, *J. Photochem. Photobiol., C.,* 2005, **6**, 264

30   G. J. Price, P. Matthias and E. J. Lenz, *Process Saf. Environ. Prot.,* 1994, **72**, 27

31   Y. Jiang, C. Pétrier and T. D. Waite, *Ultrason. Sonochem.,* 2002, **9**, 317